AMERICAN SOCIETY FOR MICROBIOLOGY | mSystems

| Genomics and Proteomics | Research Article

A comparison of short- and long-read whole-genome sequencing for microbial pathogen epidemiology

Andrea M. Schiffer,[1] Arafat Rahman,[1] Wendy Sutton,[1] Melodie L. Putnam,[1] Alexandra J. Weisberg[1]

AUTHOR AFFILIATION See affiliation list on p. 14.

ABSTRACT Whole-genome sequencing provides the highest resolution for characterizing pathogen evolution, epidemiology, and diagnostics. Genome assemblies contain information on the identity and potential phenotypes of a pathogen. Likewise, variant calling can inform on transmission patterns and evolutionary relationships. Recent improvements in Oxford Nanopore long-read sequencing have made its use attractive for genomic epidemiology. However, the accuracy and optimal strategy for analysis of Nanopore reads remain to be determined. We compared the use of Illumina short reads and Oxford Nanopore long reads for genome assembly and variant calling of phytopathogenic bacteria. We generated short- and long-read data sets for diverse phytopathogenic *Agrobacterium* strains. We then analyzed these data using multiple pipelines designed for either short or long reads and compared the results. We found that assemblies made from long reads were more complete than those made from short-read data and contained few sequence errors. Variant calling pipelines differed in their ability to accurately call variants and infer genotypes from long reads. Results suggest that computationally fragmenting long reads can improve the accuracy of variant calling in population-level studies. Using fragmented long reads, pipelines designed for short reads were more accurate at recovering genotypes than pipelines designed for long reads. Further, short- and long-read data sets can be analyzed together with the same pipelines. These findings show that Oxford Nanopore sequencing is accurate and can be sufficient for microbial pathogen genomics and epidemiology. Ultimately, this enhances the ability of researchers and clinicians to understand and mitigate the spread of pathogens.

IMPORTANCE Genome assembly and variant calling are important steps in microbial population studies and epidemiology. Most variant calling and genotyping pipelines are designed for Illumina short sequencing reads. Oxford Nanopore Technology long-read sequencing results in more complete genome assemblies but has historically been of lower quality. Here, we show that Nanopore long reads are now of sufficient quality for bacterial whole-genome assembly and epidemiology. We benchmarked the accuracy of multiple variant calling pipelines with short and long reads. Using an optimized variant calling approach, variant calls and genotypes inferred from long reads are as accurate as those inferred from short reads. Importantly, we found that gold-standard variant calling pipelines designed for short reads are also accurate with long reads when long reads are first fragmented into shorter sequences. This finding allows researchers to incorporate the advantages of Nanopore sequencing for genome assembly while maintaining high accuracy in epidemiology and population analyses.

KEYWORDS variant calling, genome assembly, genotyping, epidemiology, nanopore

Whole-genome sequencing (WGS) has driven major advances in understanding plant and clinical pathogen evolution, epidemiology, and diagnostics (1–4).

Editor Mehrad Hamidian, University of Technology Sydney, Sydney, New South Wales, Australia

Address correspondence to Alexandra J. Weisberg, Alexandra.Weisberg@oregonstate.edu.

A.R. and A.J.W. received funding from Oxford Nanopore Technologies to travel to a conference and present research findings.

See the funding table on p. 15.

Received 7 October 2025
Accepted 21 October 2025
Published 12 November 2025

Whole-genome sequences can be used to infer host range, antimicrobial resistance, and other characteristics of microbial plant and clinical pathogens. WGS data are advantageous because they simultaneously provide the highest resolution for epidemiological analysis and the characterization of pathogen transmission patterns. Recent technological developments have made it possible for plant and clinical diagnostic clinics to incorporate these tools into their arsenal. These data have already informed on emerging pathogens, such as the recent outbreak of multidrug-resistant *Pseudomonas aeruginosa* in contaminated eye drops and the introduction of *Xanthomonas hortorum* pv. *pelargonii* into the United States on geranium (5, 6).

Traditionally, short-read Illumina sequencing has been considered the gold standard for whole-genome sequencing. Illumina sequencing produces reads with high accuracy, which can be used to assemble genomes with high consensus sequence confidence or for whole-genome variant calling (7). However, Illumina reads are at most 300 bp in length, which limits their use in assembling repetitive regions of genomes. Therefore, most genome assemblies made from short reads are fragmented into multiple pieces, called contigs. Chromosome structure or the presence of mobile genetic elements, such as plasmids, can be difficult to infer from short-read assemblies.

The introduction of long-read sequencing aimed to resolve many of the issues inherent to short-read sequencing. Oxford Nanopore sequencing has the advantage of producing very long reads, up to a megabase in length, and on sequencers that are affordable to most labs. However, previous studies found that the quality of Nanopore reads was not high enough to be used on their own (8, 9). Nanopore reads also contained homopolymer repeat errors that can result in indels in assemblies (8, 10). Therefore, short-read sequencing data were often necessary for polishing long-read assemblies (11). However, recent advances in Oxford Nanopore chemistry and basecalling have changed the landscape of long-read sequencing. Assemblies produced from Nanopore long reads are now nearly perfect for many organisms (12).

Epidemiology and pathogen transmission can be characterized to the highest resolution using whole-genome variant calling. Variant calling pipelines typically use the alignment of reads to a common reference genome to identify single-nucleotide polymorphisms (SNPs) for each strain (13). Strains differing by less than a determined threshold, often 10–15 SNPs, are then grouped into genotypes (14). Mapping host or location information onto genotypes can then be used to characterize pathogen transmission. Short-read data has long been used for variant calling, and mature tools are available for this analysis (15–17). However, the historically poor quality of long reads has meant that their value and use in variant calling are not well characterized. Tools for variant calling with Nanopore reads are now available (18).

In this study, we assessed the quality of long reads in genome assembly and variant calling for population-level genotyping analysis. We compared genome assemblies made from either short or long reads. We also compared different strategies for variant calling using tools designed for either Illumina or Nanopore reads. We analyzed the consistency of variant calls produced from short and long reads of the same strain. We also assessed the ability of each pipeline to correctly group short- and long-read data from the same strain, or pairs of strains known to be identical, into the same genotype. Finally, we highlight the potential benefits that plant and medical clinics can derive from adding whole-genome sequencing to their pathogen diagnostic testing.

RESULTS

To test the viability of long-read sequencing for bacterial epidemiology, we analyzed 116 putative *Agrobacterium* strains isolated from plant samples submitted to the OSU Plant Clinic. We also included strains from the Larry Moore and Thomas Burr culture collections and from the California Department of Food and Agriculture (CDFA) collection. These 116 strains were selected to maximize diversity in plant host, location, and year of isolation (Table S1). We generated Illumina short-read data for all strains and Oxford Nanopore long-read data for a random subset of 35 strains and analyzed them independently using

multiple established pipelines. The 35 paired data sets allowed us to compare standard pipelines using short reads with assembly and variant calling pipelines using long reads. The accuracy and completeness of each approach were assessed using multiple metrics.

We first assessed the quality of short- and long-read data sets. The average read length of Nanopore reads was 6,835 bp (mean N50 read length 13,385 bp; Table S2). The average coverage for Illumina read data sets varied from 22× to 106× (mean 52× coverage), and average coverage for Nanopore read data sets varied from 17× to 173× (mean 61× coverage; Table S2). During this study, multiple Nanopore basecalling models were released. Therefore, reads were rebasecalled and retested in the pipeline. We compared the "SUP" versions of production model v4.2.0, a beta-release bacterial methylation-aware model (hereafter "bacmethyl"), and the latest production model v5.0.0. The quality of reads was consistent or improved with each new model, particularly with v5.0.0 (Table S2). Nanopore simplex reads basecalled with the v5.0.0 SUP model had an average quality score of Q19.12, corresponding to a per-read accuracy of ~98.7%.

Assemblies made with Nanopore data reveal complete chromosome structure

Genomes were assembled from either short- or long-read data, or a hybrid approach combining both, and then compared to assess completeness and accuracy (19–21). As expected, genomes assembled from long-read data or hybrid data were more complete and had higher N50 values than those assembled from short reads (Fig. 1A and B; Table S3). The average N50 was 483,620 bp for short-read SPAdes assemblies and 3,784,004 bp for long-read Flye assemblies. Short-read data sets assembled into an average of 55 contigs (Table S3). In contrast, nearly all long-read assemblies contained structurally complete chromosomes and plasmids, if present (Table S3). Total assembly size was comparable between all assemblies, but Flye and hybrid assemblies were generally slightly larger (Table S3).

Improved basecalling reduces assembly errors in long read-only assemblies

Genomes assembled from long reads have historically contained many single-nucleotide polymorphism (SNP) and small insertion/deletion (indel) errors (22). However, recent improvements in Nanopore basecalling models have reduced this error rate. We assessed the number of assembly errors in each long-read assembly by polishing with high-quality Illumina short reads and counting the number of changes made (11).

Assemblies made from reads basecalled with the most recent model (v5.0.0) had the fewest assembly errors (Table S4). Long-read assemblies with at least 50× coverage had, on average, 23 SNP errors, with as few as three errors. The number of errors in long-read assemblies declined with increasing sequencing depth of long reads (Fig. 1C). Strains with less than 30× long-read coverage had many errors, while strains with >30× sequencing depth had fewer errors (mean 43 errors). Above 80× long-read coverage, the number of errors did not dramatically decrease as sequencing depth increased. We also tested the effectiveness of polishing long-read assemblies with long reads using Medaka (23). Medaka polishing slightly reduced the number of assembly errors when long-read data sets were >80× coverage (Fig. 1C; Table S4).

We noticed an unusually high number of errors in the assembly of strain CG160, despite this sample having >100× long-read coverage. We identified low levels of contamination in the short and long reads of this sample. This contamination primarily affected the assembly of one plasmid, which contained nearly all assembly errors. Manual examination of read alignments revealed that errors were in conserved plasmid replication and conjugation loci. After filtering reads that mapped to the contaminants, a new assembly made from the filtered reads reduced the errors from 469 to 24 (Table S4).

We next identified motifs in long-read assemblies associated with errors. Previous studies found that errors in Nanopore reads occur more frequently near methylated nucleotides (24). Bacterial DNA is often methylated at specific sequence motifs (25). The motifs "GANTC" and "GATC" are methylated as part of cell cycle regulation in many

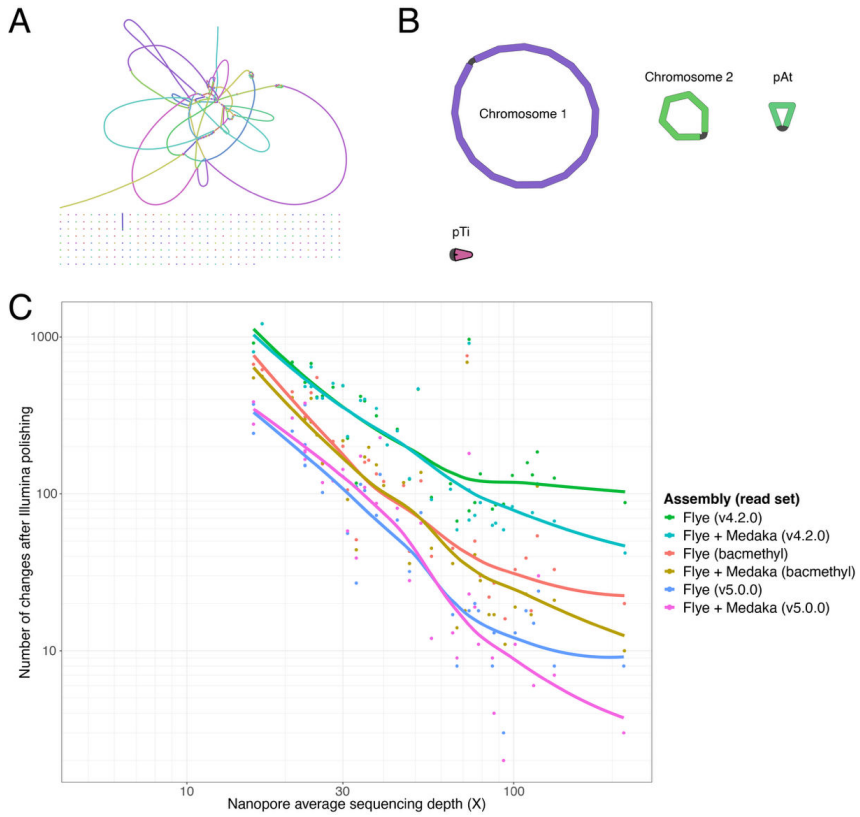

FIG 1 Nanopore-only assemblies with sufficient depth of sequencing are complete and have few errors. Assembly graphs of strain CG154 assembled from (A) Illumina short reads or (B) Nanopore long reads. (C) Assemblies of sequenced strains plotted as points on a graph of long-read sequencing depth (×) by the number of changes made to that assembly following Polypolish polishing with Illumina short reads. The long-read assembly method (Flye or Flye with Medaka polishing) and basecalling model version (v4.2.0, beta methylation-aware bacteria model [bacmethyl], or v5.0.0) are indicated by color. A best-fit line was plotted for each assembly method and model combination using locally estimated scatterplot smoothing.

Alphaproteobacteria and Gammaproteobacteria, respectively (26–28). Sequence motifs targeted by restriction-modification (R-M) defense systems are also methylated (29, 30). We characterized the sequence context around errors in long-read assemblies and identified conserved motifs (Table S5). Most assembly SNP errors occur near sites likely to be targeted for methylation. Nearly all identified motifs are either known to be methylated in agrobacteria, such as "GANTC," or are short palindromes that resemble R-M system methylation targets, such as "CTGCAG." Overall, assembly errors were reduced in data sets made from basecalling models that account for methylation (bacmethyl, v5.0.0) relative to models that do not (v4.2.0; Fig. 1C; Table S4). Most improvements in assembly error rates are in sites with predicted methylated motifs (Table S5). Other assembly errors were identified as small indels or homopolymer errors, although these also were reduced with more recent basecalling models (Table S4).

We compared gene annotations from SPAdes short-read assemblies, unpolished and short-read polished Flye long-read assemblies, and Unicycler hybrid assemblies to characterize the quality of gene calls. Flye assemblies, both polished and unpolished, consistently had slightly greater numbers of annotated gene features than SPAdes assemblies (Fig. S1). There were few or no differences in the number of genes called between polished and unpolished Flye assemblies (Table S3; Fig. S1). BUSCO scores were comparable across all read-type and assembly methods (Table S3; Fig. S2).

SNP calling pipelines vary in accuracy when used with long-read data

We next compared short and long reads for whole-genome variant calling using a variety of pipelines. We tested four SNP calling pipelines with short reads and v5.0.0 long reads. Three of the pipelines, GATK, Graphtyper, and Bcftools, were originally designed for Illumina short-read data (15–17). The other tool, Clair3, is the only one specifically designed for variant calling of Nanopore reads (18). We previously found Graphtyper to be the most consistently accurate for inferring clonal genotypes of bacterial pathogens from short-read data (31, 32). GATK was also accurate if data sets were first partitioned into below species-level groups. While neither tool was designed for long reads, we tested these pipelines with our short- and long-read data sets. We then assessed the consistency of variant calls across short and long read data sets.

The analyzed strains represent genetically diverse agrobacteria (Fig. S3). The newly sequenced strains belong to multiple species and represent each of the major pathogen lineages within the agrobacterium/rhizobium complex. Variant calling was initially performed within species-level groups (ANI >95%) and with the quality filtering thresholds recommended by each pipeline. For each strain, short and long reads were analyzed separately in each pipeline, along with strains from NCBI. We then compared the number of SNPs to the reference inferred for each strain with either short- or long-read data (Fig. 2A; Table S6).

Overall, all pipelines called roughly comparable numbers of SNPs relative to the reference for each strain with short- and full-length long reads (Fig. 2B). However, each pipeline differed in how consistently calls were made with each read type. Bcftools and Clair3 consistently called more SNPs with full-length long reads than with short reads for each strain (Fig. 2A and C). In contrast, Graphtyper consistently called fewer variants with full-length long reads than with short reads. GATK called similar numbers of variants with either short or full-length long reads. When considering only comparisons where strains are closely related to the reference genome (<300 SNPs), all pipelines produced largely consistent SNP calls using either short-read or full-length long-read data (Fig. 2A inset).

Fragmented long reads are comparable to short reads in variant calling pipelines

To more closely approximate variant calling with short reads, we fragmented full-length long reads into either 150 bp or 400 bp sequences, aligned them to reference genomes, and called variants using each pipeline. Fragmentation of long reads led to more consistent SNP calls with short reads for Graphtyper, GATK, and Bcftools, but not for Clair3 (Fig. 2; Tables S7 through S10). Variant calling using 400 bp fragments was most consistent with calls for short-read data when using Graphtyper or GATK, while variant calling with 150 bp fragments was most consistent when using Bcftools. Variant calling with Graphtyper or GATK pipelines using 400 bp long-read fragments, Bcftools with 150 bp long-read fragments, and Clair3 with full-length long reads most closely matched short-read SNP calls (Fig. 2A and 4).

We initially hypothesized that poor read mapping of full-length long reads to distantly related reference genomes was responsible for the under-calling of variants with some pipelines. However, the mapped read depth, breadth, and quality of full-length reads was not significantly worse than those of 400 bp fragmented reads across data sets (Fig. S5). In fact, all mapping statistics were slightly better with full-length reads relative to fragmented reads in nearly all data sets (Table S11). Therefore, we hypothesized that pipelines designed for short reads were unable to correctly handle long reads. To test this, we fragmented full-length mapped reads in place into 400 bp fragments, retaining the exact mapping position and quality of each sub-sequence of the full-length read alignment. Variant calls produced by Graphtyper with 400 bp split-in-place long reads were comparable to variant calls for individually mapped 400 bp read fragments (Table S10). Variant calls for both split-in-place and independently mapped 400 bp read fragments were more consistent with variant calls for short reads than with those full-length long reads (Table S10).

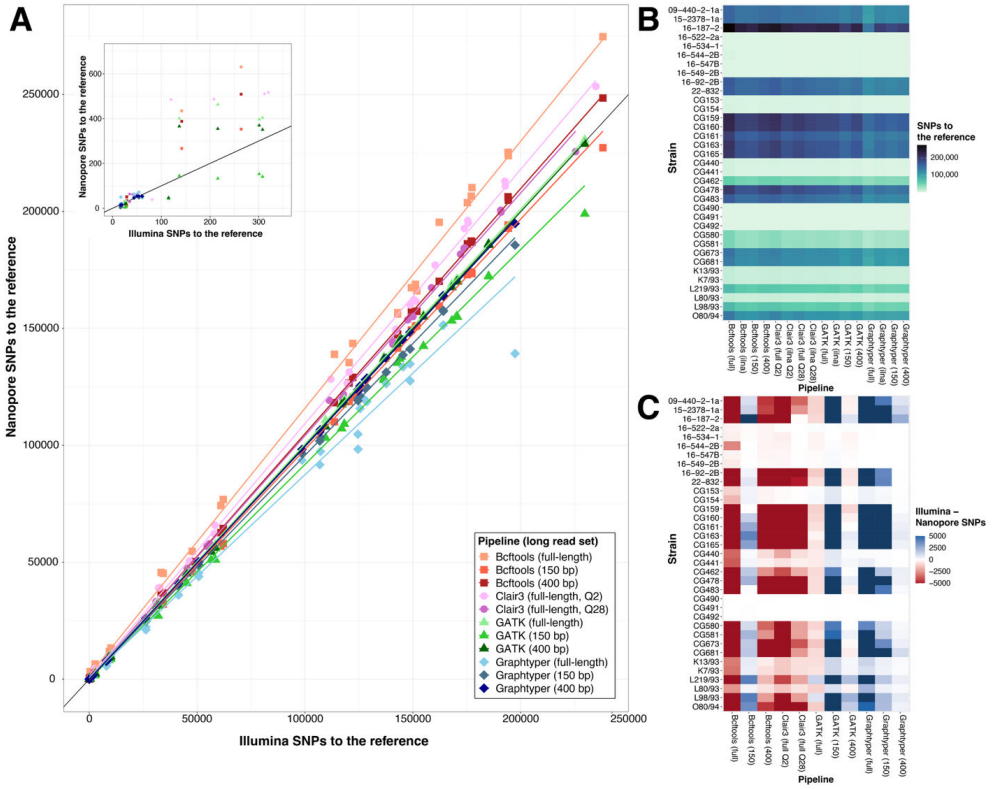

FIG 2 Comparison of variant calling pipelines. (A) Plot of SNP calls to the reference for Illumina vs Nanopore reads for each strain and pipeline. Each point represents an individual strain; shape and color indicate variant calling pipeline and long-read data set type, respectively. Long reads were either full length or fragmented into 150 bp (150) or 400 bp (400) pieces. Quality filtering for Clair3 was performed with either a threshold of QUAL >2 (Q2) or QUAL >28 (Q28). The black line represents a predicted 1 to 1 ratio between Illumina SNPs to the reference and Nanopore SNPs to the reference. The embedded graph is zoomed to show the 0 to 350 SNPs region. (B) A heatmap comparing the number of SNPs called to a reference using different variant calling pipelines and read sets. Each row is a strain, and each column is the number of SNPs called for that strain using each pipeline and read type. (C) A heatmap representing the difference in SNP calls to the reference made with Illumina and Nanopore reads for each strain. Rows are strains, and columns are variant calling pipelines and long-read type. Color indicates whether more SNPs were called with Illumina reads (blue) or Nanopore reads (red). Values greater than 5000 SNP differences are shown in dark red and dark blue.

Variant calling with Clair3 is improved by more stringent quality filtering

To infer the accuracy of variant calls with long reads, we calculated precision, recall, and F1 scores for each pipeline. Variant calls produced from short reads with each pipeline, or from short reads with Graphtyper, were used as truth sets. Variant calls produced by each pipeline from either full-length or fragmented long reads were used as the test set. Precision vs recall curves of variant calls across all strains were used to identify optimal filtering thresholds for each pipeline and read set (Fig. S6 and S7). Using the same pipeline with short reads as the truth set, most pipelines had little variation in precision or recall across thresholds (Fig. S6). However, Clair3 had a maximized precision and recall at a median threshold of QUAL > ~28. Therefore, we also included Clair3 with a QUAL > 28 variant filtering threshold in all further comparisons (Table S13). Precision vs recall curves made using Graphtyper with short reads as the truth set were largely consistent with the analyses using within-pipeline truth sets (Fig. S7).

Different long read sets are most accurate with each pipeline

We next compared the overall precision, recall, and F1 scores across pipelines and read sets (Fig. 3). When using the same pipeline as a truth set, Graphtyper with 400 bp reads

had significantly greater precision than all other pipelines, except for GATK with 400 bp reads (Kruskal–Wallis test *P*-value < $2.2*10^{-16}$, Dunn's *post-hoc* test; Fig. 3; Table S12). Graphtyper with 400 bp reads also had significantly greater F1 scores than all other pipelines, except for GATK with 400 bp reads and Clair3 with full-length reads and a filtering threshold of QUAL > 28 (Kruskal–Wallis test *P*-value < $2.6*10^{-14}$, Dunn's *post-hoc* test; Fig. 3). Recall scores were not significantly different across most pipelines and read sets. Graphtyper had comparable precision with either full-length or 400 bp reads, but significantly lower recall and F1 scores with full-length reads (Kruskal–Wallis test *P*-value < $2.2*10^{-16}$, Dunn's *post-hoc* test). Graphtyper with 400 bp long reads had a median precision of 99.2%, median recall of 98.5%, and median F1 of 98.8%. GATK with 400 bp long reads had a median precision of 97.8%, median recall of 95.9%, and median F1 of 96.1%. Clair3 with full-length reads and a QUAL > 28 filtering threshold showed a median precision of 95%, a median recall of 99.2%, and a median F1 of 96.9%.

When variant calls produced by Graphtyper using short reads were used as a truth set, Graphtyper with either full-length or 400 bp reads showed significantly better precision than all other pipelines (Kruskal–Wallis test *P*-value < $2.2*10^{-16}$; Fig. 3). Graphtyper with 400 bp reads had significantly better F1 scores than all other pipelines and read sets, including Graphtyper with full-length reads (Kruskal–Wallis test *P*-value < $2.2*10^{-16}$, Dunn's *post-hoc* test). Graphtyper with 400 bp reads had significantly better recall than all other pipelines, except for Bcftools with 150 bp reads (Kruskal–Wallis test *P*-value < $2.2*10^{-16}$, Dunn's *post-hoc* test; Fig. 3). All other pipelines had similar precision, recall, and F1 scores.

Long reads are sufficient for accurately inferring genotypes

We next compared pipelines for inferring genotypes from SNP data. Genotyping, the identification of genetically identical strains, is important for characterizing outbreaks and understanding pathogen transmission (14, 33). For each pipeline or approach, we characterized whether short- and long-read data sets for the same strain were correctly inferred to be the same genotype in 95% ANI population-level analyses. A threshold of ≤15 relative pairwise SNP differences was used to infer that two strains belong to the same genotype. Graphtyper with 400 bp long reads correctly paired the most pairs of short- and long-read data sets into genotypes (Table S14). Graphtyper correctly inferred short-read and 400 bp long-read data, fragmented either in-place or pre-mapping, from the same strain into genotypes for 18 and 16 of 35 strains, respectively. Graphtyper with full-length or 150 bp fragments correctly inferred 4 and 14 of 35 same-strain genotypes with short reads, respectively. GATK with full-length reads or any fragmented read type correctly inferred 8 and 7 genotypes, respectively. Clair3 with full-length reads and a QUAL > 28 filtering correctly inferred the same genotype for 8 of 35 strains. Clair3, using a filtering threshold of QUAL > 2, correctly inferred genotyped for 3 of 35 strains, whereas Bcftools, with either full-length or 400 bp reads, correctly inferred genotypes for only 2 of 35 strains.

While Graphtyper with 400 bp long-read fragments correctly paired short and long reads into genotypes for most strains, it did not group all. We hypothesized that this may be due to comparing strains to distantly related references. Using a 95% ANI threshold, strains with 5–7 Mb genomes can be grouped with those that differ by ~100,000 SNPs. Therefore, we tested partitioning the strains into groups using a 99% ANI threshold. We tested Graphtyper and Clair3 with these groupings (Tables S15 and S16). While some strains could not be analyzed because the 99% ANI threshold grouped them as singletons, Graphtyper correctly grouped short-read and 400 bp long-read data sets for 26 of 28 strains (Tables S14 and S15). Clair3 with a filtering threshold of QUAL > 28 correctly grouped short-read and full-length long-read data sets for 11 of 28 strains (Tables S14 and S16).

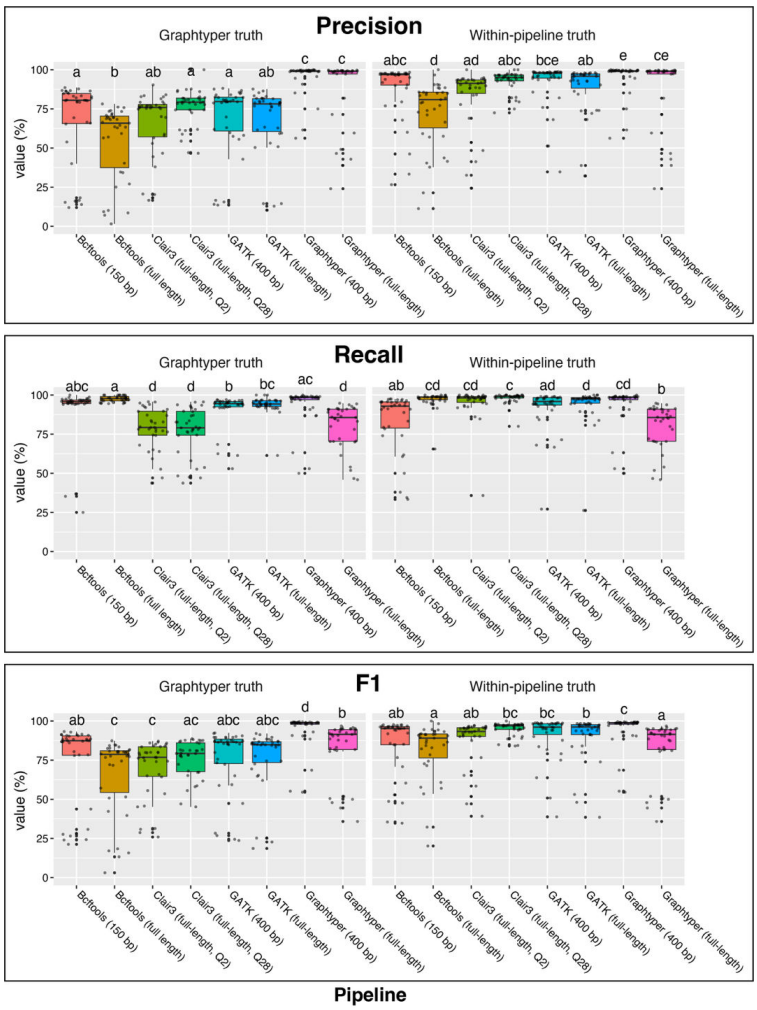

FIG 3 Variant calling accuracy across pipelines. Precision, recall, and F1 scores for per-strain variant calls produced by each pipeline using either full-length or fragmented long reads. Truth sets were defined as either variant calls produced by Graphtyper from Illumina short reads or variant calls produced by the tested pipeline using Illumina short reads. Scores are represented as percentages. Scores for each strain are represented as points and summarized as boxplots colored by data set. Significance letters from a Dunn's *post-hoc* test are displayed above each boxplot.

Pipelines differ in their ability to correctly genotype known identical strains

We next characterized how consistently each pipeline grouped different strains into genotypes. We identified 20 pairs of strains that are nearly identical (≤15 pairwise SNPs) based on alignment of short reads from one strain to the assembly of the other and calling variants with Graphtyper (Table S17). We identified 19 of the same strain pair genotypes when Clair3 with full-length long reads, using a QUAL > 2 filtering, was used instead (Table S17). However, the final strain pair, K13/93 and K7/93, was found to be nearly identical when a filtering threshold of QUAL > 28 was used (Table S17). Therefore, we used these 20 strain pairs as truth set genotypes. We then characterized the ability of each pipeline to correctly genotype these strains with either short or long reads mapped to distant reference genomes in 95% ANI population-level analyses (Table S18).

Graphtyper with either short reads or 400 bp fragmented long reads correctly genotyped the most known strain pairs, identifying 17 of 20 truth-set genotypes (Tables S10 and S18). Graphtyper with 150 bp fragments or full-length reads correctly inferred 16 and 3 genotypes, respectively. The next most accurate pipeline was Clair3 with long

reads and a filtering threshold of QUAL > 28, which correctly inferred genotypes for 15 strains (Tables S13 and S18). Clair3 with long reads and QUAL > 2 filtering inferred 11 truth set genotypes (Tables S8 and S18). GATK correctly inferred 7 truth set genotypes with either full-length or 150 bp fragmented reads (Tables S9 and S18). Bcftools with any long read data set correctly inferred 1 truth set genotype (Tables S7 and S18). Bcftools with short reads correctly inferred 9 truth set genotypes. Genotypes were inferred by comparing strains sequenced with the same technology and read type. However, pipelines varied in their ability to correctly infer known genotypes for strains sequenced using different technologies (Table S19). In most cases, comparisons made across short- and long-read data sets were consistent with results from comparisons made within read types for each pipeline.

When a 99% ANI threshold was used to group strains, Graphtyper with either short reads or 400 bp fragmented long reads correctly genotyped 19 of 20 truth-set genotypes (Tables S15 and S18). In this analysis, the final pair, strains L98/93 and L219/93, had >50,000 SNPs to the chosen reference genome and were inferred to differ by ~27 SNPs (Table S15, group 723). Clair3 with full-length reads or short reads and a quality filter of QUAL > 28 correctly genotyped 17 and 16 of 20 truth-set genotypes, respectively (Tables S16 and S18).

Epidemiology of plant clinic strains

Once we had identified an optimal pipeline and strategy for variant calling, we characterized the identity and inferred transmission patterns for the newly sequenced strains. The 116 sequenced strains are genetically diverse and represent each of the major lineages of agrobacteria (Fig. S3). Many strains are closely related to previously sequenced agrobacteria from other hosts or locations. Most strains carry oncogenic plasmids, suggesting that they are likely to be pathogenic. Genotypes inferred from the Graphtyper analysis of strains partitioned using a 99% ANI threshold were visualized as minimum spanning networks (Fig. 4; Table S15). Both short reads and 400 bp long-read fragments were consistent in identifying epidemiological links between or within locations. Strains CG163 and CG165 belong to the same genotype but were collected from two different vineyards. These data suggest a potential transmission event or acquisition from a common source. Likewise, two non-pathogenic strains (CG159, CG160) sampled from grapevine in California in 2000 are genetically identical to a non-pathogen strain also sampled from grapevine in Oregon in 2015 (15-2141-1B). Three strains (CG159, CG160, and CG161) collected from nursery N25 in 2000 represent multiple genotypes (Fig. 4). Likewise, several genotypes of strains isolated from nursery N7 in 2022 differ by more than 30,000 SNPs (Fig. 4). Both examples represent co-occurring infections at a single location.

DISCUSSION

These results, along with other recent studies, suggest that Nanopore long reads are now of sufficient quality to be used for genome assembly and variant calling independently (8, 34–37). With the latest basecalling models and sufficient depth of sequencing, long reads can be used to assemble complete genomes with very few errors. The most serious errors are indel errors, as these can cause apparent frameshift mutations that disrupt gene annotation. However, these errors are also reduced in reads produced by the latest basecalling models (Table S4). While long-read assemblies are likely of acceptable quality on their own, shallow Illumina sequencing can also be added to ensure perfect assemblies (12). However, for most use cases, this may not be necessary. Long-read assemblies are sufficient for identifying an organism, inferring phylogenetic relationships, and characterizing the presence of virulence genes or genes involved in antimicrobial resistance (AMR).

Our variant calling results are comparable to previous studies, but we identified different pipelines as most accurate (34, 35, 37). These differences are likely due to several factors, including the inclusion of different pipelines, such as Graphtyper and

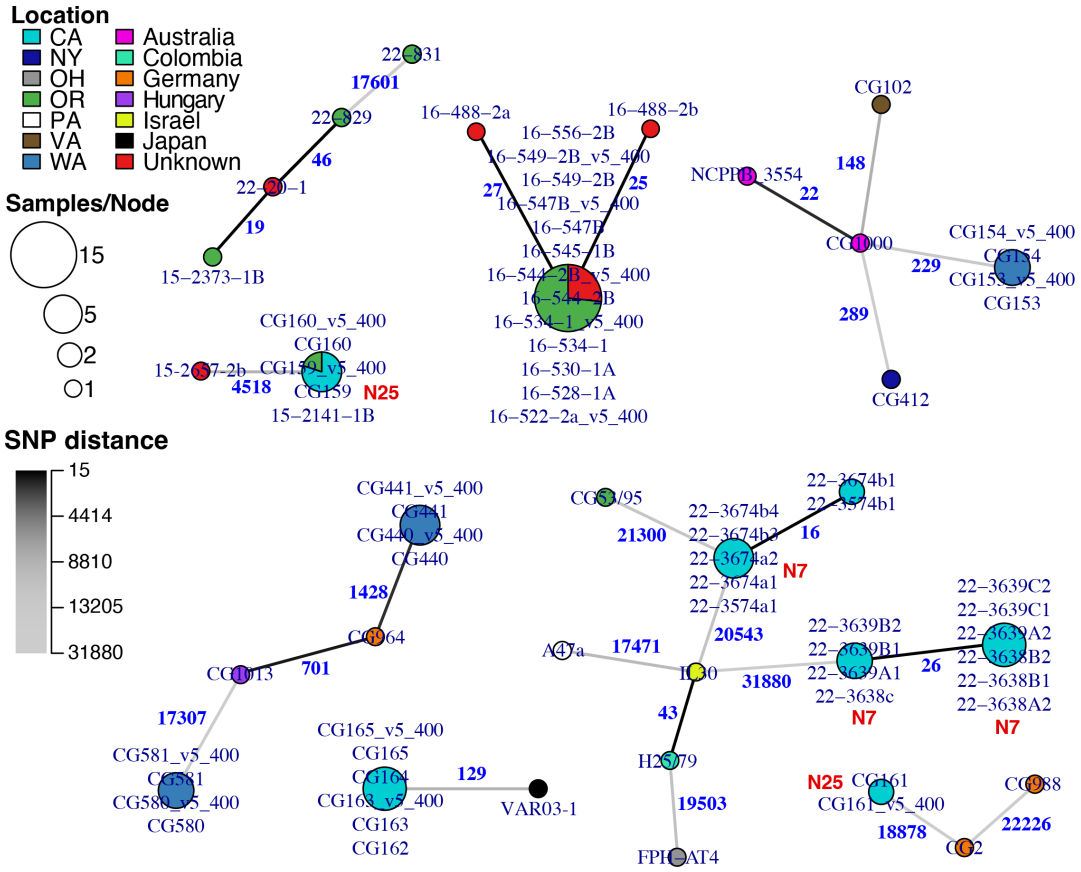

FIG 4 Whole-genome sequencing data reveals epidemiological patterns. Minimum spanning networks representing relationships between select strains. Nodes represent whole-genome genotypes inferred from strains with ≤15 SNP differences. Edge labels and color represent the number of SNP differences between genotypes. Node size indicates the number of strains of each genotype, and the proportion of each color indicates the location of isolation (country or U.S. state) for strains of that genotype. Genotypes from select nurseries are labeled in red text. Strains were analyzed in groups with >99% ANI similarity. Genotypes were inferred from variant calls produced by Graphtyper with either short or 400 bp long read data (labeled "_v5_400").

GATK. Previous studies used closely related reference genomes (34, 35, 37). In this study, we tested data sets representing population-level studies rather than performing a direct comparison of strains known to be nearly identical. Other studies introduced simulated genomic changes in sequenced strains to use as truth-set variants (37). In this study, strains were sequenced with both Illumina and Nanopore technologies, and variants produced from short reads were used as the truth set. It is possible that long reads may identify additional true variants that are not captured by short reads, particularly in repetitive regions (37). To avoid this, we identified pairs of strains that are identical in direct comparisons with short and long reads. These strain-pair genotypes served as an additional truth set that is robust to this potential issue. Tested pipelines with the greatest precision and recall also recovered the greatest number of known strain-pair genotypes in population-level analyses. Pipelines that use pangenome graphs, such as Graphtyper, had the greatest consistency in calling variants across strains when using a distant reference genome (16).

Results from this study show that fragmenting Nanopore reads into shorter sequences is important for ensuring accurate variant calling using pipelines designed for short reads. All short-read pipelines produced more accurate variant calls when long reads were first fragmented into shorter sequences (Fig. 3). Once long reads were fragmented, pipelines designed for short reads were as accurate as, or more accurate than, tools designed for long reads. The reduced accuracy with full-length reads is not likely due to poor mapping of full-length reads to a distant reference, as mapping quality

statistics for full-length long reads were comparable to fragmented reads (Fig. S5; Table S11). Importantly, fragmenting mapped full-length reads "in place" resulted in nearly identical variant calls compared with pre-fragmented reads (Table S10). These "in-place" fragmented read alignments have identical reference coverage and read depth as the full-length read alignments, yet variant calls were much improved. This suggests that these variant calling differences are likely due to an inability of pipelines designed for short reads to correctly analyze long reads. Modifying these tools to support long reads would allow users to use the most accurate tools without losing the information present in full-length reads. For now, fragmentation can be performed prior to or after read mapping to promote accurate variant calling.

Previous studies found the long-read pipeline Clair3 to be the most accurate variant caller with long reads (37). For our data sets, Clair3 was among the top variant calling tools, but only when a more stringent variant filtration threshold was used (Fig. 2B; Table S7). Using Clair3 with the developer-recommended filtering threshold of QUAL > 2 resulted in a larger number of false positive variants and the recovery of fewer truth-set genotypes (Fig. 2C and 3; Table S18). This was especially the case when variants were called to a distant reference. Once a more stringent filtering threshold of QUAL > 28 was used, Clair3 with full-length reads achieved accuracy comparable to short-read pipelines with fragmented long reads. However, variant calls produced by Clair3 from short reads recovered few truth-set genotypes at either filtering threshold (Table S18).

Most variant calling tools are only designed for either short or long reads. Few tools explicitly have options for mixed data sets. This results in compromises when choosing parameters or settings for each run. For example, using long reads with Graphtyper requires setting an option that ignores filtering by read pair mapping ("--no_filter_on_proper_pairs"). If a Graphtyper analysis has strains with paired short reads and other strains with long reads, read pairing will be ignored for the short-read data sets. This parameter did not dramatically impact variant calling with short reads in our analyses; however, it may be a problem for other data sets. Pipelines that include per-sample options for either short or long reads could improve results for mixed data sets. Alternatively, users should use only one read type or the other.

Caution should be taken when interpreting variant calls and genotypes inferred from mixed data sets of short and long reads. In some cases, comparisons across data types did not correctly infer a genotype for strain pairs, whereas comparisons within data type did. For example, using Graphtyper and 95% ANI groups, analyses of 400 bp long-read or short-read data for strains CG153 and CG154 inferred that they belonged to the same genotype (Tables S10 and S18). However, when comparing across technologies, the 400 bp long-read data of CG154 were not genotyped with the short-read data of strain CG153 (Tables S10 and S19). However, by grouping strains using a 99% ANI threshold, we eliminated most issues with genotyping across read types. In this analysis, short- and long-read data correctly grouped CG153 with CG154 in all comparisons (Fig. 4; Table S19). We recommend using Graphtyper with fragmented long reads for characterizing mixed data sets. Clair3 with more stringent filtering is also accurate when only long-read data are used.

Using a higher ANI threshold or identifying sub-lineages to select closer reference genomes may improve variant calling and genotyping (32, 38). Even at a 99% ANI threshold, strains can differ by >40,000 SNPs. We observed several cases where a 99% ANI threshold is still too distant for accurate variant calling. For example, using strain CA75/95 as reference for 99% ANI group 723, the short and long reads of strains L219/93 and L98/93 did not genotype together (Table S18). However, when variants were instead called using L219/93 as reference, the read sets and strains were genotyped together as expected (Table S18). If strains appear to be closely related but not the same genotype, we recommend re-analyzing with a reference genome more closely related to those strains.

Generating whole-genome data is now easier and less expensive than before. Individual labs or plant clinics can prepare libraries and perform Illumina short-read

or Oxford Nanopore long-read sequencing in the lab with relative ease. These results suggest that either technology is sufficient for genome assembly and variant calling in most cases. Both Illumina and Oxford Nanopore have released DNA sequencers that can be purchased by individual labs. An advantage of long-read sequencing is that libraries are generally less time-consuming and easier to prepare in the lab. If sequencing is performed in-house, costs can be cheaper, and results acquired more quickly than with short-read sequencing. Rapid advances in sequencing technology provide a major opportunity for plant clinics and labs to generate data with the highest resolution for diagnostics and epidemiology.

MATERIALS AND METHODS

Genome sequencing and analysis

Strains were selected from the Larry Moore culture collection or from those collected by the OSU Plant Clinic (Table S1). Additional strains were shared by the California Department of Food and Agriculture (CDFA). Strains were cultured in MGYs liquid media or plates at 28°C (39). The Promega Wizard Genomic DNA Extraction Kit (Promega; Madison, WI) was used to extract DNA from cell pellets of each strain. The protocol was modified to include an overnight lysis step at 37°C, with mixing achieved by inverting the tube rather than pipetting. All strains were sequenced with both Illumina and Oxford Nanopore technologies. The SeqWell PurePlex Kit was used to prepare libraries for Illumina sequencing. Illumina libraries were sequenced (2 × 150 bp) on an Illumina MiniSeq (Illumina; San Diego, California) in the OSU Plant Clinic. The Rapid Barcoding 96V14 Kit (SQK-RBK114.96) was used to prepare multiplexed libraries for Nanopore sequencing. Nanopore libraries were sequenced on an R10.4.1 PromethION flow cell using a P2 Solo sequencer (Oxford Nanopore; Oxford, UK). Dorado v.0.5.0, with the default parameters, SUP basecalling, and different basecalling models, was used to basecall Nanopore reads (40).

FastQC was used to check Illumina reads for quality (41). NanoPlot v1.42.0 with the default parameters was used to check Nanopore reads for quality (42). Spades v3.15.3, with the parameters "--phred-offset 33 –careful -k 21,33,55,77,99," was used to assemble genomes from Illumina reads only (20). For all assemblies, contigs with <500 bp in length or <5× coverage were removed. Flye v2.9.2-b1786 with the parameters "--scaffold --read-error 0.03" was used to assemble genomes from only Nanopore reads only (19). Medaka v.2.0.0 with the model r1041_e82_400bps_sup_v4.2.0 or r1041_e82_400bps_sup_v5.0.0 was used to polish Flye assemblies (23). Polypolish v0.5.0 with the default parameters was used to polish Flye assemblies with Illumina reads (11). Unicycler v0.5.0 with the parameter "--mode normal" was used to create a hybrid assembly from both Illumina and Nanopore reads (21). Beav v0.2 with the parameter "--agrobacterium" and Bakta v.1.8.2 were used to annotate genomes (43, 44). BUSCO with the parameters "-m genome -l rhizobium-agrobacterium_group_odb10," Quast v5.0.0 with the default parameters, and the Samtools v.1.19.2 subcommand "depth" were used to gather genome assembly statistics (15, 45, 46). MEME v5.4.1 with the parameters "-dna -nmotifs 10" was used to identify motifs around putative Flye assembly errors detected by Polypolish polishing (47). Motifs were filtered to those with an evalue < 1. Bandage v.0.8.1 with the default parameters was used to visualize assembly graphs (48). FastANI v1.1 with the default parameters was used to calculate pairwise average nucleotide identity (ANI) and cluster strains into groups based on 95% or 99% thresholds (49).

The assembly of strain CG160 was found to have an unusual number of errors. BBTools sendsketch.sh v39.06 with the default parameters was used to identify contaminants (50). Sourmash v4.8.11 sketch and compare were used to generate and compare signatures for the contaminated plasmid and the plasmids of a closely related strain (51). BBTools seal.sh v39.06 with the parameters "pattern = out_%.fq ambig = first" along with combined reference assemblies was used to filter out contaminated

reads (50). The assemblies of *Rhizobium rhizogenes* K84 (NCBI: GCF_000016265.1), *Rhizobium tumorigenes* B21/90 (NCBI: GCF_019355815.1), CG160 without the contaminated plasmid, and the equivalent plasmid from closely related strain CG159 were used as input to partition reads. Non-contaminant reads mapping to the CG160 assembly and CG159 plasmid were combined and used in the previously described analyses.

Phylogenetic analysis

NCBI data sets were used to download all publicly available genomes of the *Agrobacterium*/*Rhizobium* complex from NCBI on 19 July 2023 (52). Automlsa2 v0.8.1 with the parameters "--allow_missing 4 --missing_check," was used to generate a maximum likelihood multi-locus sequence analysis (MLSA) phylogeny including newly sequenced and NCBI strains (53, 54). The protein sequences AcnA, AroB, CgtA, CtaE, DnaK, GlgB1, GlyS, HemF, LeuS, LysC, MurC, PrfC, RecR, RplB, RpoB, RpoC, SecA, SMc00019, SMc00714, SMc01147, SMc01148, SMc02059, SMc02478, ThrA, and TruA from *Sinorhizobium meliloti* strain 1021 were used as references (55). IQ-TREE2 v2.2.0 with parameters "-m MFP -B 1000 -alrt 1000 --msub nuclear --merge rclusterf" was used to generate a maximum likelihood phylogeny (56). The R package ggtree was used to plot phylogenies (57).

Whole-genome SNP calling and comparisons

Whole-genome SNP analyses were performed using Illumina short reads, full-length Nanopore reads, or fragmented Nanopore reads. All newly sequenced strains, including those with short reads or both short and long reads, and strains downloaded from NCBI were analyzed together. Seqkit v0.16.1 sliding with parameters "-W 150 -s 150" or "-W 400 -s 400" was used to split Nanopore reads into 150 bp and 400 bp fragments, respectively (58). Species groups were determined by single-linkage clustering of ANI values of short-read-only, hybrid, or NCBI assemblies, using minimum ANI thresholds of 95% or 99% (49). Within species groups/lineages, references were selected among hybrid or NCBI assemblies based on assembly completeness, as determined by a low number of contigs and a high N50. Kingfisher v0.2.2 subcommand "get" and parameters "-m ena-ascp aws-http prefetch" were used to download Illumina reads for NCBI strains (59). Bwa v0.7.17-r1188 mem with the parameter "-M" was used to map Illumina reads to a reference within each group (60). Minimap2 v2.26-r1175 with parameter "-ax map-ont" was used to map Nanopore reads to a reference within each group (61). Samtools v1.19.2 with the subcommand view and parameter "-F 256" was used to retain only primary alignments for mapped long reads (15). For the fragmented in-place analysis, a custom Python script was used to fragment mapped long reads "in-place" into 400 bp sequences, maintaining all mapping information and quality from the original alignment.

The developer-suggested parameters and filtering thresholds were used for each tested pipeline. GATK v4.6.2.0 HaplotypeCaller with the parameters "-ERC GVCF -ploidy 1 -allowPotentiallyMisencodedQuals" was used to call variants for each data set (17). GATK CombineGVCFs and GenotypeGVCFs with the default parameters were used to combine partial variant calls across strains. GATK SelectVariants with parameter "-selectType SNP" was used to select SNP variants only. GATK VariantFiltration with parameter "--filter-Expression QD < 2.0 SOR > 3.0 QUAL < 30.0 FS > 60.0 MQ < 40.0 MQRankSum < -12.5 ReadPosRankSum -8.0" was used to hard-filter SNPs. The GATK tool SelectVariants was used with parameter "--excludefiltered" to remove filtered SNPs. Graphtyper v2.7.3 with the parameter "--no_filter_on_proper_pairs," was used to call SNPs (16). The GATK VariantFiltration tool with parameters "-G-filter 'isHet == 1' -g-filter-name 'isHetFilter' --set-filtered-genotype-to-no-call'" was used to filter heterozygous calls from Graphtyper vcf files. The vcflib program vcffilter with parameters "-f 'ABHet < 0.0 | ABHet > 0.33' -f 'ABHom < 0.0 | ABHom > 0.97' -f 'MaxAASR > 0.4' -f 'MQ > 30'" was used to filter Graphtyper variant calls for quality (62). Bcftools v1.17 mpileup with parameters "-x -I -Q 13 -h 100 -M 10000 -a 'INFO/SCR,FORMAT/SP,INFO/ADR,INFO/ADF," subcommand call with parameters "-m -ploidy 1 -V indels," and the apply_filters.py script with parameters "-q 27 -M 55 -V 0.00001 x 0.2 -K 0.9 -s 1 -d 5" were used to call SNPs and filter for

quality (15, 36). Clair3 v.1.0.4 with parameters "--no_phasing_for_fa --include_all_ctgs --haploid_precise –gvcf" and either "--platform='ont' --model_path="${CONDA_PREFIX}/bin/models/r1041_e82_400bps_sup_v500"" or "--platform='ilmn' --model_path="${CONDA_PREFIX}/bin/models/ilmn"" for Nanopore or Illumina reads, respectively, were used to call SNPs (18). Bcftools merge with the parameter "-0" was used to merge Clair3 gvcf files. The vcflib program vcffilter with parameters "-f 'QUAL > 2'" or "-f 'QUAL > 28'" was used to filter Clair3 variant calls for quality. The R package poppr v.2.9.5 was used to calculate pairwise SNP distances and plot minimum spanning networks (33). Bcftools view with the parameter "--samples," was used to extract individual strain SNP calls for both short reads and long reads fragmented into 400 bp. These files were filtered to only contain non-reference SNP calls.

To identify truth-set genotypes, the short- or full-length long reads of each strain were mapped individually to the hybrid assembly of all other strains, along with reads of that reference, and used to call variants. Bwa and Graphtyper with the above-described parameters were used to align and call variants with short reads (16, 60). Similarly, minimap2 and Clair3, using the above-described parameters, were used to map full-length long reads and call variants for the same comparisons (18, 61). Variant calls were filtered as described above. Strain pairs where the short or long reads of both strains were inferred to have fewer than 15 pairwise differences were considered to be a genotype.

Variant calling accuracy and consistency across technologies were then characterized for the 35 strains with both Illumina and Nanopore reads from the above-described analyses. VCFCompare v.1.0 was used to calculate overall precision and accuracy scores (63). Vcfdist v2.5.2 with the parameters "--max-qual 60 --min-qual 0 --cluster gap 50" and Illumina SNPs as the truth data set were used to calculate accuracy scores for Nanopore SNPs across quality thresholds (64). For precision vs recall curves, true positives, true negatives, false positives, and false negatives were each summed across the 35 strains at each quality score threshold to calculate precision and recall. The R package FSA was used to perform the Kruskal–Wallis test followed by a Dunn's test with Holm method *P*-value adjustment, to assess statistical significance of precision and recall between pipelines (65).

ACKNOWLEDGMENTS

The authors would like to thank the California Department of Food and Agriculture (CDFA) for sharing *Agrobacterium* strains. The authors thank the Department of Botany and Plant Pathology for supporting the CQLS high-performance computing infrastructure.

This work was supported by startup funds from the Department of Botany and Plant Pathology at Oregon State University. This project was funded in part by USDA NIFA through the Western Integrated Pest Management Center, award SA 18-4060-41, and by the National Institute of General Medical Sciences of the National Institutes of Health under award number 1R35GM160469.

AUTHOR AFFILIATION

[1]Department of Botany and Plant Pathology, Oregon State University, Corvallis, Oregon, USA

AUTHOR ORCIDs

Andrea M. Schiffer http://orcid.org/0009-0008-7372-9616
Arafat Rahman http://orcid.org/0000-0003-4222-9615
Alexandra J. Weisberg http://orcid.org/0000-0002-0045-1368

FUNDING

Funder	Grant(s)	Author(s)
National Institute of General Medical Sciences	1R35GM160469	Andrea M. Schiffer Arafat Rahman Wendy Sutton Melodie L. Putnam Alexandra J. Weisberg
National Institute of Food and Agriculture	SA 18-4060-41	Wendy Sutton Melodie L. Putnam

DATA AVAILABILITY

Final genome assemblies and raw read data were uploaded to NCBI under BioProject PRJNA1255661. All genome assemblies and scripts for this project can be found in the following GitHub repository: https://github.com/weisberglab/nanopore_quality_manuscript. Variant calling vcf files for each data set are also available in the following Zenodo repository: https://doi.org/10.5281/zenodo.17518122.

ADDITIONAL FILES

The following material is available online.

Supplemental Material

Supplemental Figures (mSystems01426-25-s0001.pdf). Figures S1 to S7.
Supplemental Tables (mSystems01426-25-s0002.xlsx). Tables S1 to S19.

REFERENCES

1. Everhart S, Gambhir N, Stam R. 2021. Population genomics of filamentous plant pathogens-a brief overview of research questions, approaches, and pitfalls. Phytopathology 111:12–22. https://doi.org/10.1094/PHYTO-11-20-0527-FI
2. McLeish MJ, Fraile A, García-Arenal F. 2021. Population genomics of plant viruses: the ecology and evolution of virus emergence. Phytopathology 111:32–39. https://doi.org/10.1094/PHYTO-08-20-0355-FI
3. Parkhill J, Wren BW. 2011. Bacterial epidemiology and biology--lessons from genome sequencing. Genome Biol 12:230. https://doi.org/10.1186/gb-2011-12-10-230
4. Straub C, Colombi E, McCann HC. 2021. Population genomics of bacterial plant pathogens. Phytopathology 111:23–31. https://doi.org/10.1094/PHYTO-09-20-0412-RVW
5. Grossman MK, Rankin DA, Maloney M, Stanton RA, Gable P, Stevens VA, Ewing T, Saunders K, Kogut S, Nazarian E, et al. 2024. Extensively drug-resistant *Pseudomonas aeruginosa* outbreak associated with artificial tears. Clin Infect Dis 79:6–14. https://doi.org/10.1093/cid/ciae052
6. Iruegas-Bocardo F, Weisberg AJ, Riutta ER, Kilday K, Bonkowski JC, Creswell T, Daughtrey ML, Rane K, Grünwald NJ, Chang JH, Putnam ML. 2023. Whole genome sequencing-based tracing of a 2022 introduction and outbreak of *Xanthomonas hortorum* pv. *pelargonii*. Phytopathology 113:975–984. https://doi.org/10.1094/PHYTO-09-22-0321-R
7. Goodwin S, McPherson JD, McCombie WR. 2016. Coming of age: ten years of next-generation sequencing technologies. Nat Rev Genet 17:333–351. https://doi.org/10.1038/nrg.2016.49
8. Luan T, Commichaux S, Hoffmann M, Jayeola V, Jang JH, Pop M, Rand H, Luo Y. 2024. Benchmarking short and long read polishing tools for nanopore assemblies: achieving near-perfect genomes for outbreak isolates. BMC Genomics 25:679. https://doi.org/10.1186/s12864-024-10582-x
9. Sereika M, Kirkegaard RH, Karst SM, Michaelsen TY, Sørensen EA, Wollenberg RD, Albertsen M. 2022. Oxford Nanopore R10.4 long-read sequencing enables the generation of near-finished bacterial genomes from pure cultures and metagenomes without short-read or reference polishing. Nat Methods 19:823–826. https://doi.org/10.1038/s41592-022-01539-7
10. Huang Y-T, Liu P-Y, Shih P-W. 2021. Homopolish: a method for the removal of systematic errors in nanopore sequencing by homologous polishing. Genome Biol 22:95. https://doi.org/10.1186/s13059-021-02282-6
11. Wick RR, Holt KE. 2022. Polypolish: short-read polishing of long-read bacterial genome assemblies. PLoS Comput Biol 18:e1009802. https://doi.org/10.1371/journal.pcbi.1009802
12. Wick RR, Judd LM, Holt KE. 2023. Assembling the perfect bacterial genome using Oxford Nanopore and Illumina sequencing. PLoS Comput Biol 19:e1010905. https://doi.org/10.1371/journal.pcbi.1010905
13. Olson ND, Lund SP, Colman RE, Foster JT, Sahl JW, Schupp JM, Keim P, Morrow JB, Salit ML, Zook JM. 2015. Best practices for evaluating single nucleotide variant calling methods for microbial genomics. Front Genet 6:235. https://doi.org/10.3389/fgene.2015.00235
14. Stimson J, Gardy J, Mathema B, Crudu V, Cohen T, Colijn C. 2019. Beyond the SNP threshold: identifying outbreak clusters using inferred transmissions. Mol Biol Evol 36:587–603. https://doi.org/10.1093/molbev/msy242
15. Danecek P, Bonfield JK, Liddle J, Marshall J, Ohan V, Pollard MO, Whitwham A, Keane T, McCarthy SA, Davies RM, Li H. 2021. Twelve years of SAMtools and BCFtools. Gigascience 10:giab008. https://doi.org/10.1093/gigascience/giab008
16. Eggertsson HP, Jonsson H, Kristmundsdottir S, Hjartarson E, Kehr B, Masson G, Zink F, Hjorleifsson KE, Jonasdottir A, Jonasdottir A, Jonsdottir I, Gudbjartsson DF, Melsted P, Stefansson K, Halldorsson BV. 2017. Graphtyper enables population-scale genotyping using pangenome graphs. Nat Genet 49:1654–1660. https://doi.org/10.1038/ng.3964
17. McKenna A, Hanna M, Banks E, Sivachenko A, Cibulskis K, Kernytsky A, Garimella K, Altshuler D, Gabriel S, Daly M, DePristo MA. 2010. The genome analysis toolkit: a MapReduce framework for analyzing next-generation DNA sequencing data. Genome Res 20:1297–1303. https://doi.org/10.1101/gr.107524.110

18. Zheng Z, Li S, Su J, Leung A-S, Lam T-W, Luo R. 2022. Symphonizing pileup and full-alignment for deep learning-based long-read variant calling. Nat Comput Sci 2:797–803. https://doi.org/10.1038/s43588-022-00387-x
19. Kolmogorov M, Yuan J, Lin Y, Pevzner PA. 2019. Assembly of long, error-prone reads using repeat graphs. Nat Biotechnol 37:540–546. https://doi.org/10.1038/s41587-019-0072-8
20. Prjibelski A, Antipov D, Meleshko D, Lapidus A, Korobeynikov A. 2020. Using SPAdes *de novo* assembler. Curr Protoc Bioinform 70. https://doi.org/10.1002/cpbi.102
21. Wick RR, Judd LM, Gorrie CL, Holt KE. 2017. Unicycler: resolving bacterial genome assemblies from short and long sequencing reads. PLoS Comput Biol 13:e1005595. https://doi.org/10.1371/journal.pcbi.1005595
22. Delahaye C, Nicolas J. 2021. Sequencing DNA with nanopores: troubles and biases. PLoS One 16:e0257521. https://doi.org/10.1371/journal.pone.0257521
23. Oxford Nanopore Technologies. 2023. Medaka. Available from: https://github.com/nanoporetech/medaka
24. Chiou C-S, Chen B-H, Wang Y-W, Kuo N-T, Chang C-H, Huang Y-T. 2023. Correcting modification-mediated errors in nanopore sequencing by nucleotide demodification and reference-based correction. Commun Biol 6:1215. https://doi.org/10.1038/s42003-023-05605-4
25. Sánchez-Romero MA, Casadesús J. 2020. The bacterial epigenome. Nat Rev Microbiol 18:7–20. https://doi.org/10.1038/s41579-019-0286-2
26. Gonzalez D, Kozdon JB, McAdams HH, Shapiro L, Collier J. 2014. The functions of DNA methylation by CcrM in *Caulobacter crescentus*: a global approach. Nucleic Acids Res 42:3720–3735. https://doi.org/10.1093/nar/gkt1352
27. Kahng LS, Shapiro L. 2001. The CcrM DNA methyltransferase of *Agrobacterium tumefaciens* is essential, and its activity is cell cycle regulated. J Bacteriol 183:3065–3075. https://doi.org/10.1128/JB.183.10.3065-3075.2001
28. Palmer BR, Marinus MG. 1994. The dam and dcm strains of *Escherichia coli*--a review. Gene 143:1–12. https://doi.org/10.1016/0378-1119(94)90597-5
29. Vasu K, Nagaraja V. 2013. Diverse functions of restriction-modification systems in addition to cellular defense. Microbiol Mol Biol Rev 77:53–72. https://doi.org/10.1128/MMBR.00044-12
30. Williams RJ. 2003. Restriction endonuclease. Mol Biotechnol 23:225–243. https://doi.org/10.1385/mb:23:3:225
31. Weisberg AJ, Davis EW, Tabima J, Belcher MS, Miller M, Kuo C-H, Loper JE, Grünwald NJ, Putnam ML, Chang JH. 2020. Unexpected conservation and global transmission of agrobacterial virulence plasmids. Science 368:eaba5256. https://doi.org/10.1126/science.aba5256
32. Weisberg AJ, Grünwald NJ, Savory EA, Putnam ML, Chang JH. 2021. Genomic approaches to plant-pathogen epidemiology and diagnostics. Annu Rev Phytopathol 59:311–332. https://doi.org/10.1146/annurev-phyto-020620-121736
33. Kamvar ZN, Tabima JF, Grünwald NJ. 2014. Poppr: an R package for genetic analysis of populations with clonal, partially clonal, and/or sexual reproduction. PeerJ 2:e281. https://doi.org/10.7717/peerj.281
34. Bloomfield M, Bakker S, Burton M, Castro ML, Dyet K, Eustace A, Hutton S, Macartney-Coxson D, Taylor W, White RT. 2024. Resolving a neonatal intensive care unit outbreak of methicillin-resistant *Staphylococcus aureus* to the SNV level using Oxford Nanopore simplex reads and HERRO error correction. bioRxiv. https://doi.org/10.1101/2024.07.11.603154
35. Bogaerts B, Van den Bossche A, Verhaegen B, Delbrassinne L, Mattheus W, Nouws S, Godfroid M, Hoffman S, Roosens NHC, De Keersmaecker SCJ, Vanneste K. 2024. Closing the gap: Oxford Nanopore Technologies R10 sequencing allows comparable results to Illumina sequencing for SNP-based outbreak investigation of bacterial pathogens. J Clin Microbiol 62:e01576-23. https://doi.org/10.1128/jcm.01576-23
36. Hall MB, Rabodoarivelo MS, Koch A, Dippenaar A, George S, Grobbelaar M, Warren R, Walker TM, Cox H, Gagneux S, Crook D, Peto T, Rakotosamimanana N, Grandjean Lapierre S, Iqbal Z. 2023. Evaluation of Nanopore sequencing for *Mycobacterium tuberculosis* drug susceptibility testing and outbreak investigation: a genomic analysis. Lancet Microbe 4:e84–e92. https://doi.org/10.1016/S2666-5247(22)00301-9
37. Hall M.B, Wick RR, Judd LM, Nguyen AN, Steinig EJ, Xie O, Davies M, Seemann T, Stinear TP, Coin L. 2024. Benchmarking reveals superiority of deep learning variant callers on bacterial nanopore sequence data. eLife 13:RP98300. https://doi.org/10.7554/eLife.98300.3
38. Castillo-Ramírez S. 2024. On the road to genomically defining bacterial intra-species units. mSystems 9:e00584-24 https://doi.org/10.1128/msystems.00584-24
39. Moore LW, Chilton WS, Canfield ML. 1997. Diversity of opines and opine-catabolizing bacteria isolated from naturally occurring crown gall tumors. Appl Environ Microbiol 63:201–207. https://doi.org/10.1128/aem.63.1.201-207.1997
40. Oxford Nanopore Technologies. 2024. Dorado. Available from: https://github.com/nanoporetech/dorado
41. Andrews S. 2024. FastQC: a quality control tool for high throughput sequence data. Available from: https://www.bioinformatics.babraham.ac.uk/projects/fastqc/
42. Rademakers R, Coster W. 2023. NanoPack2: population-scale evaluation of long-read sequencing data. Bioinformatics 39:btad311. https://doi.org/10.1093/bioinformatics/btad311
43. Jung JM, Rahman A, Schiffer AM, Weisberg AJ. 2024. Beav: a bacterial genome and mobile element annotation pipeline. mSphere 9:e00209-24. https://doi.org/10.1128/msphere.00209-24
44. Schwengers O, Jelonek L, Dieckmann MA, Beyvers S, Blom J, Goesmann A. 2021. Bakta: rapid and standardized annotation of bacterial genomes via alignment-free sequence identification. Microb Genom 7:000685. https://doi.org/10.1099/mgen.0.000685
45. Gurevich A, Saveliev V, Vyahhi N, Tesler G. 2013. QUAST: quality assessment tool for genome assemblies. Bioinformatics 29:1072–1075. https://doi.org/10.1093/bioinformatics/btt086
46. Simão FA, Waterhouse RM, Ioannidis P, Kriventseva EV, Zdobnov EM. 2015. BUSCO: assessing genome assembly and annotation completeness with single-copy orthologs. Bioinformatics 31:3210–3212. https://doi.org/10.1093/bioinformatics/btv351
47. Bailey TL, Elkan C. 1994. Fitting a mixture model by expectation maximization to discover motifs in biopolymers. Proc Int Conf Intell Syst Mol Biol 2:28–36.
48. Wick RR, Schultz MB, Zobel J, Holt KE. 2015. Bandage: interactive visualization of *de novo* genome assemblies. Bioinformatics 31:3350–3352. https://doi.org/10.1093/bioinformatics/btv383
49. Jain C, Rodriguez-R LM, Phillippy AM, Konstantinidis KT, Aluru S. 2018. High throughput ANI analysis of 90K prokaryotic genomes reveals clear species boundaries. Nat Commun 9:5114. https://doi.org/10.1038/s41467-018-07641-9
50. Bushnell B. 2024. BBMap. Available from: https://sourceforge.net/projects/bbmap
51. Titus Brown C, Irber L. 2016. Sourmash: a library for MinHash sketching of DNA. JOSS 1:27. https://doi.org/10.21105/joss.00027
52. O'Leary NA, Cox E, Holmes JB, Anderson WR, Falk R, Hem V, Tsuchiya MTN, Schuler GD, Zhang X, Torcivia J, Ketter A, Breen L, Cothran J, Bajwa H, Tinne J, Meric PA, Hlavina W, Schneider VA. 2024. Exploring and retrieving sequence and metadata for species across the tree of life with NCBI Datasets. Sci Data 11:732. https://doi.org/10.1038/s41597-024-03571-y
53. Davis E. 2023. automlsa2 (0.81). Available from: https://github.com/davised/automlsa2
54. Davis II EW, Weisberg AJ, Tabima JF, Grunwald NJ, Chang JH. 2016. Gall-ID: tools for genotyping gall-causing phytopathogenic bacteria. PeerJ 4:e2222. https://doi.org/10.7717/peerj.2222
55. Zhang YM, Tian CF, Sui XH, Chen WF, Chen WX. 2012. Robust markers reflecting phylogeny and taxonomy of rhizobia. PLoS One 7:e44936. https://doi.org/10.1371/journal.pone.0044936
56. Minh BQ, Schmidt HA, Chernomor O, Schrempf D, Woodhams MD, von Haeseler A, Lanfear R. 2020. IQ-TREE 2: new models and efficient methods for phylogenetic inference in the genomic era. Mol Biol Evol 37:1530–1534. https://doi.org/10.1093/molbev/msaa015
57. Yu G, Smith DK, Zhu H, Guan Y, Lam T-Y. 2017. Ggtree: an R package for visualization and annotation of phylogenetic trees with their covariates and other associated data. Methods Ecol Evol 8:28–36. https://doi.org/10.1111/2041-210X.12628
58. Shen W, Le S, Li Y, Hu F. 2016. SeqKit: a cross-platform and ultrafast toolkit for FASTA/Q file manipulation. PLoS One 11:e0163962. https://doi.org/10.1371/journal.pone.0163962
59. Woodcroft BJ, Cunningham M, Gans JD, Bolduc BB, Hodgkins SB. 2024. Kingfisher: a utility for procurement of public sequencing data. Zenodo. https://zenodo.org/records/10525139.
60. Li H. 2013. Aligning sequence reads, clone sequences and assembly contigs with BWA-MEM. arXiv. https://doi.org/10.48550/arXiv.1303.3997

61. Li H. 2018. Minimap2: pairwise alignment for nucleotide sequences. Bioinformatics 34:3094–3100. https://doi.org/10.1093/bioinformatics/bty191
62. Garrison E, Kronenberg ZN, Dawson ET, Pedersen BS, Prins P. 2022. A spectrum of free software tools for processing the VCF variant call format: vcflib, bio-VCF, cyvcf2, hts-nim and slivar. PLoS Comput Biol 18:e1009123. https://doi.org/10.1371/journal.pcbi.1009123
63. Nkambule L. 2023. VCFCompare. Available from: https://github.com/LindoNkambule/VCFCompare
64. Dunn T, Narayanasamy S. 2023. Vcfdist: accurately benchmarking phased small variant calls in human genomes. Nat Commun 14:8149. https://doi.org/10.1038/s41467-023-43876-x
65. Ogle D, Doll J, Wheeler AP, Dinno A. 2025 FSA: simple fisheries stock assessment methods (R package version 0.10.0). Available from: https://CRAN.R-project.org/package=FSA